POTENTIAL FIRE DETECTION BASED ON KALMAN-DRIVEN CHANGE DETECTION

[†]*F. van den Bergh*

[†]Remote Sensing Research Unit
Meraka Institute
Pretoria, South Africa
fvdbergh@csir.co.za

[†,‡]*G. Udahemuka,* [‡]*B. J. van Wyk*

[‡]French South African Technical Institute in Electronics
Tshwane University of Technology
Pretoria, South Africa
gudahemuka@csir.co.za, vanwykb@tut.ac.za

ABSTRACT

A new active fire event detection algorithm for data collected with the Spinning Enhanced Visible and Infrared Imager (SEVIRI) sensor, based on the extended Kalman filter, is introduced. Instead of using the observed temperatures of the spatial neighbours of a pixel to detect anomalous temperatures, the new algorithm only considers previous observations at the current pixel. The algorithm harnesses the Kalman filter to obtain a prediction of the expected brightness temperature at a given location, which is then compared to the actual SEVIRI observation. An adaptive threshold is used to determine whether the observed difference is indicative of a potential fire event. Initial tests show that the performance of this method is comparable to that of the EUMETSAT FIR product.

***Index Terms*—** Fires, Nonlinear detection

1. INTRODUCTION

Geostationary sensors, such as the SEVIRI instrument found on the Meteosat Second Generation (MSG) satellites, allow the monitoring of earth surface properties at a high temporal resolution. This high temporal update rate allows for the construction of a brightness temperature profile referred to as the Diurnal Temperature Cycle (DTC), which enables the development of a promising type of fire event detection algorithm. In this paper, a change detection algorithm is proposed which detects abnormal increases in temperature in the observed DTC; these increases are typically indicative of fire events. This approach considers an individual pixel without taking into account the condition of its neighbouring pixels, in contrast with the typical contextual fire detection algorithms.

Two different change detection algorithms are compared: one based on the Kalman filter, and another based on the extended Kalman filter. The Kalman filters are used to predict brightness temperatures one step ahead; the difference between the observed and predicted temperatures can then be used to flag potential fires.

Section 2 briefly discusses related active fire detection algorithms that have been developed for SEVIRI data. The formulation of the new extended Kalman filter based algorithm is presented in Section 3, followed by comparative results in Section 4, and concluding remarks in Section 5.

2. BACKGROUND

The SEVIRI instrument has a 3.9 μm channel, which is well suited to observing temperatures in the range of the earth's surface temperature, which implies that this channel can reveal regions with abnormally high temperatures. Several active fire detection methods have been applied to SEVIRI data, with contextual algorithms appearing to be quite popular despite SEVIRI's large pixel size. These contextual methods often depend on fixed thresholds that may have to be adjusted either regionally, or seasonally, such as the approach used in the AFIS system [1]. Alternatively, conservative thresholds (different thresholds for nighttime and daytime) can be used, such as the approach used by the EUMETSAT FIR product [2, 3], but this may not yield optimal detection rates for smaller fires. Another algorithm that relies on a combination of solar zenith angle heuristics and fixed thresholds was presented by Roberts *et al.* [4].

In a departure from the contextual approach, several change detection based methods for SEVIRI have been proposed. A Kalman filter tracking approach was introduced by Van den Bergh and Frost [5]; this idea will be further developed in this paper. Another change detection based method has been introduced by Calle *et al.* [6]; their method approximates the emissivity in the 3.9 μm channel, which allows the solar contribution to be removed. After this preprocessing step, a potential fire can be detected by comparing the current brightness temperature to that of the previous day at the same time of day. Lastly, a method that directly tests the difference between successive brightness temperatures against fixed thresholds has been proposed by Laneve *et al.* [7].

This study was supported by the joint French/South African SAFeTI programme.

Table 1. Symbols used in the DTC model

Parameter	Meaning
T_0 (K)	Residual temperature (before sunrise)
T_a (K)	Temperature amplitude
ω (minutes)	Half-period of cosine term
t_m (solar time)	Time of maximum temperature
t_s (solar time)	Start of decay function
τ (minutes)	Attenuation constant
δT (K)	$T_0 - T(t \to \infty)$ where t represents time

3. METHOD

3.1. Algorithm Overview

The potential fire detection algorithm described here tracks the evolution of temperature at a given location through time. A Kalman filter [8] is used to obtain an estimate of the expected temperature using all previous observations. A test is performed to determine whether the most recently observed temperature is significantly higher than the expected temperature predicted by the Kalman filter.

The Kalman filter requires an underlying model to drive the evolution of temperature through time in the absence of observations, such as would occur during extended periods of cloud cover. In Section 3.2 a suitable model for driving the Kalman filter is introduced. Section 3.3 proceeds to describe the details of the Kalman filter fire detection algorithm.

3.2. Diurnal Temperature Cycle Model

The brightness temperature observed at a given location (*e.g.* a SEVIRI pixel) over a 24-hour period describes a curve called the *diurnal temperature cycle* (DTC). One of the models that has been proposed to approximate the shape of this curve is that of Göttsche and Olesen [9], which expresses the brightness temperature as a function of time such that

$$T(t) = T_0 + \delta T + \begin{cases} T_a \cos\left(\frac{\pi}{\omega}(t - t_m)\right) - \delta T & \text{if } t < t_s \\ \left(T_a \cos\left(\frac{\pi}{\omega}(t_s - t_m)\right) - \delta T\right) e^{-\frac{(t-t_s)}{\tau}} & \text{if } t \geq t_s, \end{cases} \quad (1)$$

with the various model parameters as described in Table 1. DTC model parameters can be obtained by fitting the model to observed data with the Nelder-Mead simplex optimization algorithm using the minimum average deviation criterion [10].

The analytical DTC model is a powerful tool to mitigate the influence of observation noise, such as that owing to atmospheric effects. Figure 1 illustrates actual SEVIRI brightness temperature observations, together with a fitted DTC model. The figure also illustrates that short segments of missing values have little impact on the ability of the model to fit the remaining observations correctly.

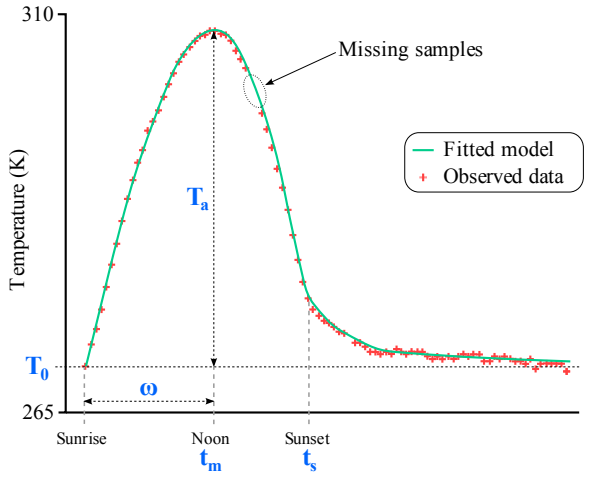

Fig. 1. SEVIRI brightness temperature observations (3.9 μm band) over a 24-hour period, with a fitted DTC model overlay.

3.3. Change Detection Algorithm

The method proposed by Van den Bergh and Frost [5] used an empirically derived DTC approximation to drive a Kalman filter. The Kalman filter models the expected temperature as a linear process, such that

$$x_k = A_{k-1} x_{k-1} + n_{k-1}, \quad (2)$$

where x_k represents the state of the system (expected temperature, in this case) at time step k, A_{k-1} is the state transition coefficient, and n_{k-1} represents the process noise. Although the filter is linear, the value of A_k is allowed to vary with k, thus the non-linear DTC is approximated as a piecewise linear function. In the original algorithm proposed by Van den Bergh and Frost [5], the $\{A_k\}$ coefficients were derived empirically from observed brightness temperature values. Potential fires were detected by testing the difference between the observed temperature and the predicted temperature against a fixed threshold (Figure 2).

The method introduced in this paper extends that method by using a more sophisticated analytical DTC model, developed by Göttsche and Olesen [9] to serve as the underlying model for the Kalman filter. The $\{A_k\}$ and process noise covariance parameters are derived from the seven most recent DTCs with realistic DTC model parameters, with A_k computed as $(m_{(k+1) \pmod{96}})/(m_{k \pmod{96}})$ where m denotes the mean DTC value derived from the seven cycles.

A second version of the algorithm replaces the Kalman filter with an *extended Kalman filter* (EKF) [11]. The extended Kalman filter models the state as

$$x_k = f(x_{k-1}, n_{k-2}) + n_{k-1}, \quad (3)$$

where f is a non-linear function. The underlying process is assumed to correspond with the analytical model of Göttsche

Table 2. Results of change detection using the standard Kalman filter (SKF) and the extended Kalman filter (EKF) at the time of the MODIS overpass, compared to the MODIS MOD14 and MYD14 fire products.

Date	MOD14+ MYD14	SKF-Change detection		EKF-Change detection	
		True Positive	Unconfirmed	True Positive	Unconfirmed
2007/07/31	645	488 (76%)	38	506 (78%)	42
2007/08/01	740	577 (78%)	39	575 (78%)	32
2007/08/02	1168	868 (74%)	45	964 (83%)	29
2007/08/03	1049	770 (73%)	16	803 (77%)	11
2007/08/04	318	231 (73%)	53	254 (80%)	55

Table 3. Results of change detection using the standard Kalman filter (SKF) and the extended Kalman filter (EKF), compared to the EUMETSAT FIR product ("probable" + "possible" FIR detections).

Date	FIR (all)	SKF-Change detection		EKF-Change detection	
		True Positive	Unconfirmed	True Positive	Unconfirmed
2007/07/31	363	253 (70%)	73	287 (79%)	65
2007/08/01	847	632 (75%)	97	664 (78%)	46
2007/08/02	895	611 (68%)	71	688 (77%)	48
2007/08/03	1339	870 (65%)	115	1004 (75%)	84
2007/08/04	196	129 (66%)	32	146 (74%)	18

and Olesen, so (1) is used directly to construct the extended Kalman filter update equations. It is expected that this non-linear formulation of the process update step in the Kalman filter will allow the filter to track the behaviour of the observed values with greater accuracy.

A residual temperature is computed at each time step by subtracting the one-timestep prediction of the Kalman filter from the observed temperature. Instead of using a fixed threshold to detect abnormally large residuals, an adaptive threshold is computed using a sliding window. The window includes residuals immediately preceding the current sample, as well as samples from a similar window at a 24-hour lag (*i.e.*, from the same time the previous day). This adaptive threshold is able to compensate for the diurnal changes in the variance of the residuals. The residuals (at each time step) were experimentally found to have a t-distribution, which is in agreement with previous experiments [5]. This distribution can be used to assign a confidence value to an observed residual, which can be used to derive an overall indication of the algorithm's confidence of detecting a potential fire.

4. RESULTS

Data collected using the SEVIRI instrument were used because of the sensor's high temporal resolution (15 minutes). MSG level 1.5 data were obtained from the EUMETSAT archive[1] over the region (20 S, 23 E) to (33 S, 38 E). The data correspond to a period spanning from 2007/07/23 to 2007/08/14. There were numerous fire events in this region during this time.

As a first experiment, the potential fire events reported by the two Kalman filter based algorithms have been compared to the fires reported by the MODIS MOD14/MYD14 fire products. Only fires reported for observations closest in time to the MODIS overpass were considered to make the comparison more meaningful. The result of this comparison is presented in Table 2. The *true positive* columns denote potential fires that were detected in SEVIRI pixels that overlapped with corresponding MODIS fire events in the MOD14/MYD14 fire product. The *unconfirmed* columns denote potential fire events that were reported by the Kalman filter based algorithms that did not correspond to active fire events in the MOD14/MYD14 product. These detections could be false positives, or they could be fire events that were missed by MOD14/MYD14 but picked up by SEVIRI right after the MODIS overpass. Validation using a burned area product is still underway, so these are considered potential false positives.

Comparisons of the Kalman-based algorithms to the EUMETSAT FIR product are presented in Tables 3 and 4. From these tables it can be seen that the extended Kalman filter is able to detect almost all the "probable" fires reported in the FIR product. The "possible" fires reported in the FIR product have not yet been confirmed with burned area products for this specific dataset, and may therefore contain some false positive detections.

[1] All MSG Data © 2007 and 2008 EUMETSAT.

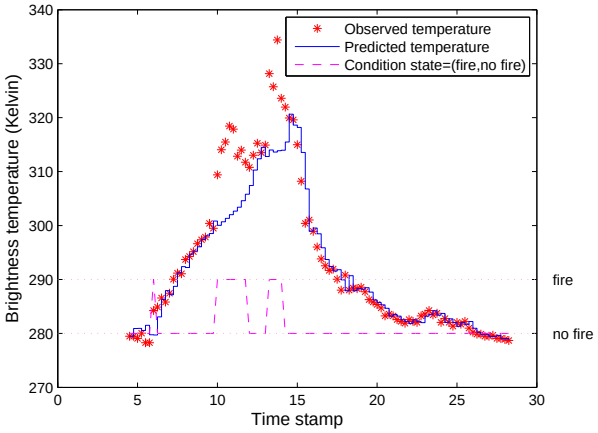

Fig. 2. An example of the Kalman filter detecting abnormally high brightness temperatures, flagged as fires here.

Table 4. Results of change detection using the standard Kalman filter (SKF) and the extended Kalman filter (EKF), compared to the EUMETSAT FIR product (only "probable" FIR detections).

Date	FIR (prob.)	SKF-CD True Positive	EKF-CD True Positive
2007/07/31	204	151 (74%)	200 (98%)
2007/08/01	515	471 (91%)	508 (99%)
2007/08/02	576	485 (84%)	534 (93%)
2007/08/03	923	794 (86%)	914 (99%)
2007/08/04	101	76 (75%)	94 (93%)

5. CONCLUSION

A new potential fire event detection algorithm, based on an extended Kalman filter driven by an analytical DTC model, was proposed. This version of the algorithm was experimentally compared to an older version based on the Kalman filter.

The extended Kalman filter algorithm was able to detect anomalies in the DTC profile, indicating potential fires, that could not be detected by the standard Kalman filter algorithm. Despite these algorithms' lower detection rate, compared to MODIS, they have the advantage of a much more frequent updates. The performance of the extended Kalman filter algorithm was demonstrated to compare favourably to the "probable" category of detections offered in the EUMETSAT FIR product.

Future work will focus on validating the *unconfirmed* detections, and optimising the adjustable parameters found in the Kalman algorithm.

6. REFERENCES

[1] P. E. Frost, H. Vosloo, D. Davis, J. Decloites, S. Kumar, and J. Schmaltz, "Development of an advanced fire information system for southern Africa," Report (africa), United Nations Environmental Program (UNEP), 2004.

[2] C. C. DaCamara, T. J. Calado, M. Amraoui, and M. C. Pereira, "The SAF for land surface analysis wildfire applications," in *Joint 2007 EUMETSAT Meteorological Satellite Conference of the American Meteorological Society*, Amsterdam, The Netherlands, Sept. 2007.

[3] EUMETSAT, *Active fire monitoring with MSG Algorithm theoretical basis document*, 1st edition, Apr. 2007, Document number: EUM/MET/REP/07/0170.

[4] G. J. Roberts and M. J. Wooster, "Fire detection and fire characterization over Africa using METEOSAT SEVIRI," *IEEE Transactions on Geoscience and Remote Sensing*, vol. 46, no. 4, pp. 1200–1218, Apr. 2008.

[5] F. van den Bergh and P. E. Frost, "A multi-temporal approach to fire detection using MSG data," in *Proceedings of Multitemp05*, Biloxi, Mississippi, May 2005, pp. 156–160.

[6] A. Calle, J. L. Casanova, and A. Romo, "Fire detection and monitoring using MSG Spinning Enhanced Visible and Infrared Imager (SEVIRI) data," *Journal of Geophysical Research*, vol. 111, pp. 1–13, 2006.

[7] G. Laneve, M. M. Castronuovo, and E. G. Cadau, "Continuous monitoring of forest fires in the Mediterranean area using MSG," *IEEE Transactions on Geoscience and Remote Sensing*, vol. 44, no. 10, pp. 2761–2768, Oct. 2006.

[8] R. E. Kalman, "A new approach to linear filtering and prediction problems," *Transactions of the ASME - Journal of Basic Engineering*, vol. 3, pp. 35–45, 1960.

[9] F.-M. Göttsche and F.-S. Olesen, "Modelling of diurnal cycles of brightness temperature extracted from METEOSAT data," *Remote Sensing of Environment*, vol. 76, pp. 337–348, 2001.

[10] F. van den Bergh, M. A. van Wyk, and B. J. van Wyk, "A comparison of data-driven and model-driven approaches to brightness temperature diurnal cycle interpolation," in *Proceeding of 17th Symposium of the Pattern Recognition Association of South Africa*, Parys, South Africa, Dec. 2006, pp. 252–256.

[11] S. Haykin, *Adaptive filter theory*, Prentice-Hall, Upper Saddle River, N.J., 4th edition, 2002.